

# INFLUENCE OF CRYSTAL THICKNESS ON REMANENT DOMAIN STRUCTURES IN COBALT. II. RECTANGULAR-PRISM-SHAPED SINGLE CRYSTALS

BY B. WYSŁOCKI

Institute of Ferrous Metallurgy, Gliwice\*

(Received May 7, 1968)

The dependence of the domain width  $D$  on the crystal thickness  $T$  in the magnetically preferred direction [0001] in cobalt is studied experimentally for the honeycomb ( $H$ ) and Goodenough ( $G$ ) remanent domain structures, on a set of single crystals in the form of rectangular prisms with square cross-sections ( $8\text{ mm} \times 8\text{ mm}$ ) in the basal plane (0001), their thickness  $T$  ranging from  $11500\text{ }\mu\text{m}$  to  $3\text{ }\mu\text{m}$ . The dependence is found to be of the form  $D_X; m = T^b a_X; m$  where  $m = 1$  for  $T \leq T_1$  and  $m = 2$  for  $T > T_1$ ,  $X = H$  or  $G$ ,  $b_1 = 0.5$ ,  $b_2 = 0.57$ , and  $T_1 = 50\text{ }\mu\text{m}$  is the critical thickness below which closure domains disappear. The results are in very good agreement with those obtained on a single wedge-shaped sample in Part I of this paper.

## 1. Introduction

In Part I of this paper [1], the influence of the crystal thickness in the magnetically preferred direction on the regular remanent domain structures in cobalt has been examined and the dependence of the domain width  $D$  on the crystal thickness  $T$  determined<sup>1</sup>. The sample used in [1] was a wedge-shaped single crystal with the dimensions  $4\text{ mm}$  and  $9\text{ mm}$  in the crystallographic directions  $[0\bar{1}10]$  and  $[\bar{2}110]$  respectively, the crystal thickness in the magnetically preferred direction [0001] decreasing linearly along the direction  $[\bar{2}110]$  from  $3\text{ mm}$  to  $2\text{ }\mu\text{m}$ . Both the regular remanent domain structures in cobalt have been examined, namely, the honeycomb ( $H$ ) and Goodenough ( $G$ ) domain structure (see models in [1, 2]). The dependence of the domain width on the crystal thickness was experimentally found to be of the form

$$D_X = T^b a(X; b), \quad [a] = [T]^{1-b} \quad (1)$$

where  $X$  denotes the type of domain structure. The value of the exponent  $b$  does not depend on  $X$  but merely on the fact whether closure domains (at the basal crystal surface) do occur

\* Address: Zakład Materiałów Magnetycznych, Instytut Metalurgii Żelaza, Gliwice, Miarki 12, Polska.

<sup>1</sup> Figures from Part I are here referred to by using the notation Fig. I. X for Fig. X from paper [1].

or not; the shape, size, number, and distribution of the closure domains has evidently no influence on  $b$ . Denoting by  $HS$ ,  $GS$  and  $HC$ ,  $GC$  the domain structures  $H$ ,  $G$  without ( $S = \text{simple}$ ) and with ( $C = \text{complex}$ ) closure domains, respectively, the results obtained in [1] show that for cobalt we have (if  $D$  and  $T$  are measured in  $\mu\text{m}$ )

$$b = 0.5 \equiv b_1, \\ a(X; b) = \begin{cases} a(HS; b_1) \equiv a_{H;1} = 1.01 \mu\text{m}^{0.5} \\ a(GS; b_1) \equiv a_{G;1} = 0.66 \mu\text{m}^{0.5} \end{cases} \quad (2)$$

for  $T \leq T_1$ , and

$$b = 0.57 \equiv b_2, \\ a(X; b) = \begin{cases} a(HC; b_2) \equiv a_{H;2} = 0.77 \mu\text{m}^{0.43} \\ a(GC; b_2) \equiv a_{G;2} = 0.50 \mu\text{m}^{0.43} \end{cases} \quad (3)$$

for  $T \geq T_1$ , where  $T_1$  is the critical crystal thickness below which the closure domains disappear and the complex domain structure becomes simple. The value of  $T_1$  depends on the material. As shown in [1],  $T_1 \cong 50 \mu\text{m}$  for cobalt. Using the above notation, the relation (1) can be written in the convenient form

$$D_{X;m} = T^{b_m} a_{X;m}, \quad m = \begin{cases} 1 & \text{for } T \leq T_1 \\ 2 & \text{for } T \geq T_1 \end{cases}, \quad [a_m] = [T]^{1-b_m} \quad (4)$$

with  $b_m$  and  $a_{X;m}$  for cobalt given<sup>2</sup> by Eqs (2) and (3).

Insofar as the results in [1] were obtained from measurements and observations on a single wedge-shaped sample, *i.e.*, on domain structures with (monotonously) *varying* domain width, the question arises whether or not they represent the "true" thickness dependence of the domain width, that is, whether or not they coincide with results obtained on plate-like single-crystalline samples, each of them having a fixed but different thickness in the magnetically preferred direction. The more so as the experimental results obtained in [1] are evidently in disagreement with theory. (See also the critique of earlier experiments by other authors given in [1, 2].)

Furthermore, the critical thickness  $T_0$ , below and above which different conditions are required to obtain the same type of domain structure, was also determined in [1] and found to be for cobalt about  $12 \mu\text{m}$  in one case, and  $80 \mu\text{m}$  in the other. This discrepancy was presumed to be attributable to the shape of the sample.

The purpose of the present paper is to settle these questions.

## 2. Observations and measurements

In the present experiment fifteen single-crystalline samples of cobalt (purity 99.46%) have been examined, each having the shape of a rectangular prism with faces perpendicular to the crystallographic directions  $[0001]$ ,  $[0\bar{1}10]$  and  $[\bar{2}110]$ , as shown in Fig. 1. The samples

<sup>2</sup> If  $D$  and  $T$  are measured in other units than  $\mu\text{m}$ , the coefficients  $a_{X;m}$  must be changed accordingly.

were cut from a single rectangular block having a square cross-section in the basal plane, the length of its sides being 8 mm. The thickness  $T$  of the samples in the magnetically preferred direction [0001] varied from 11500  $\mu\text{m}$  in the thickest sample to 3  $\mu\text{m}$  in the thinnest. The preparation of the samples (mechanical and electrolytical polishing, determination of crystallographic orientation, etc.) and the colloid used for the powder-pattern observations were the same as in [1].

Observations and measurements (taken from enlarged photographs of the powder-patterns) were performed on all faces of the samples, with the exception of the three thinnest samples where they were confined to the basal crystal surfaces. In this way measurements on the basal surface could be checked with those performed on two (opposite) axial surfaces. Due to the shape of the samples (constant  $T$ ), the measurements could in each case be extended over the whole crystal surface, the accuracy being thus better than in [1]. To test the reliability of the measurements, each domain structure has been destroyed and reproduced several times and the measurements repeated. This procedure served also as a precaution against incidental deformations of the domain structure.

The creating (saturation) magnetic field  $H_0$  used in producing the remanent domain structures was in thicker samples ( $T \geq 15 \mu\text{m}$ ) parallel to the hexagonal axis [0001] in the case of the  $H$ -structure (Figs 2a and 3a-d), and parallel to the direction  $[\bar{2}110]$  in the case of the  $G$ -structure (Figs 2b and 3e-h), the field strength being respectively 1.5 kOe and 18 kOe, and the switching-off velocity 300 Oe/sec in both cases. A representative set of powder-patterns from the crystal surfaces on which measurements were carried through, *i.e.*, from the basal surface (0001) and the axial surface ( $0\bar{1}10$ ), is shown in Figs 2 and 3, the thickness  $T$  of the samples (*cp.* Fig. 1) being 11500  $\mu\text{m}$  in Fig. 2, and (from the top) 3700  $\mu\text{m}$ , 850  $\mu\text{m}$ , 77  $\mu\text{m}$ , 15  $\mu\text{m}$  in Fig. 3.

Illustrative powder-patterns from the crystal surface ( $\bar{2}110$ ) are shown in Fig. 2. The almost identical spacing between the Bloch walls on both the axial crystal surfaces in Fig. 2a (which are orthogonal to each other) is rather surprising, as the pattern on the crystal surface ( $\bar{2}110$ ) is hardly compatible with any cross-section of the  $H$ -structure in this plane if the spacing between the lines on the axial crystal surface ( $0\bar{1}10$ ) and the distances between neighbouring hexagons on the basal surface (0001) are to be constant, *i.e.*, if  $b = 2a$  and  $c = 2a + b$  in Fig. 4, in agreement with our observations. On the other hand, there are quite distinct traces of parallel Bloch walls on the axial crystal surface ( $\bar{2}110$ ) in Fig. 2b, the spacing being evidently larger than on the axial surface ( $0\bar{1}10$ ) but coinciding with the spacing between the dagger-like closure domains along the direction  $[0\bar{1}10]$  (white circles on the basal surface (0001) in Fig. 2b). This would lead to the model of the  $G$ -structure shown in Fig. 5a. According to Fig. 5b we have

$$b = 2c \operatorname{tg} \alpha. \quad (5)$$

Assuming  $b = 1.8a$  and  $\alpha = 70^\circ$  from the observations reported in [3, 4], we obtain

$$c \approx 0.33a. \quad (6)$$

In thin samples ( $T \leq 10 \mu\text{m}$ ), the creating field  $H_0$  has to be at a proper angle with the hexagonal axis [0001] to obtain regular  $H$  or  $G$ -structures [6, 7]. These angles are:  $88^\circ$

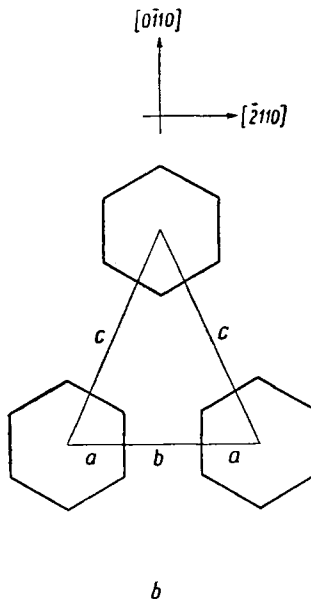
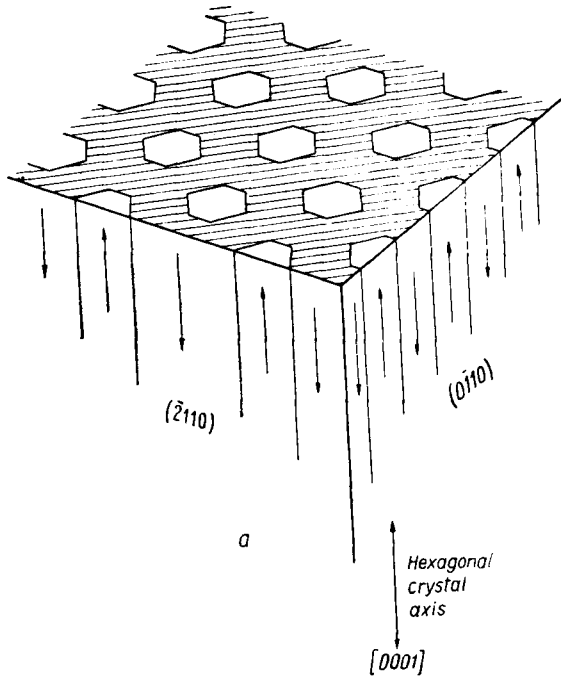


Fig. 4. Model of honeycomb ( $H$ ) domain structure. Observations show that  $c \cong 2a+b$  and  $2a \cong b$ , the latter equality being in disagreement with theory [2, 6]

or  $92^\circ$  in the first case ( $H$ -structure) and  $75^\circ$  in the latter ( $G$ -structure). Examples of domain structures obtained for the angles  $\vartheta = 0^\circ, 40^\circ, 75^\circ, 88^\circ, 90^\circ$  and  $92^\circ$  (with  $H_0$  lying in

TABLE I

$T$ [ $\mu\text{m}$ ]	$D_H$ [ $\mu\text{m}$ ]	$D_G$ [ $\mu\text{m}$ ]	$T$ [ $\mu\text{m}$ ]	$D_H$ [ $\mu\text{m}$ ]	$D_G$ [ $\mu\text{m}$ ]
11500	145	96	77	8.7	5.5
6300	101	68	50	6.5	4.4
3700	76	50	30	5	3.4
2100	54	36	15	3.6	2.4
850	32.2	21.4	10	3	2
510	24.6	16.5	5	2.1	1.4
266	17.2	11.2	3	1.7	1.1
133	11.5	7.7			

the crystallographic plane  $(\bar{2}110)$  and having a strength of 1.5 kOe for  $0 \leq \vartheta \leq 40^\circ$ ,  $140^\circ \leq \vartheta \leq 180^\circ$  and 18 kOe for  $40^\circ < \vartheta < 140^\circ$ ) are shown in Fig. 6a, b, c, d, e and f, respectively, for a crystal thickness  $T = 10 \mu\text{m}$ .

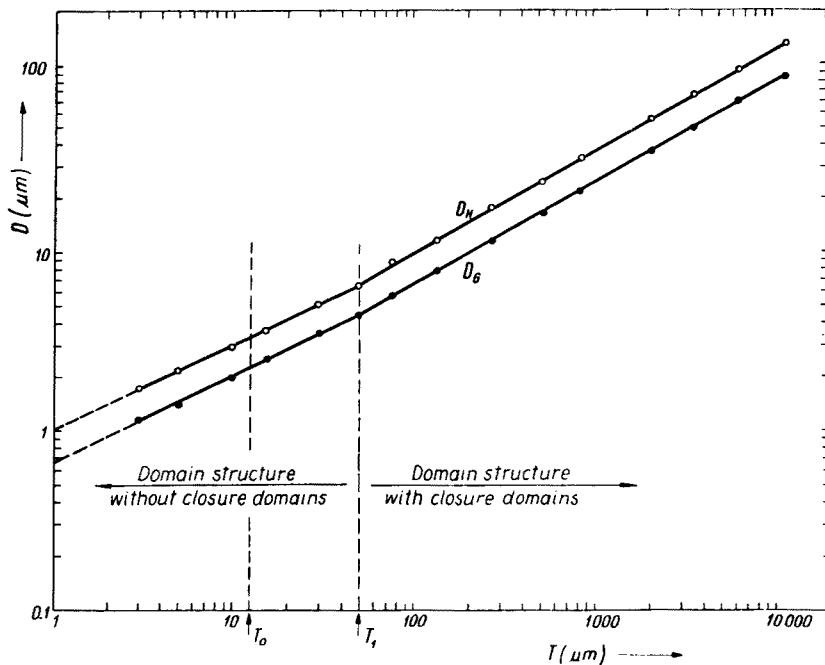


Fig. 7. Experimental curves for the dependence of the domain widths  $D_H$  ( $H$ -structure) and  $D_G$  ( $G$ -structure) on the crystal thickness  $T$  leading to the relation (4) (see [1] for comparison with theory and earlier experiments)

In view of our present results two remarks are due concerning the critical thickness  $T_0$  below and above which different conditions are required to obtain the remanent  $H$  and  $G$ -structures. Firstly, in crystals with constant  $T$  this thickness appears to be the same for both the

domain structures and  $T_0 \approx 12 \mu\text{m}$  for cobalt. Hence, the result  $T'_0 \approx 80 \mu\text{m}$  obtained in one case in [1] must be attributed to the particular shape of the sample used in [1], as expected. Secondly, the requirement that  $\vartheta$  must be equal to  $88^\circ$  (or  $92^\circ$ ) and  $75^\circ$  to obtain the  $H$  and  $G$ -structures, respectively, in thin crystals ( $T < T_0$ ) is not necessarily true for samples with varying thickness, as these domain structures were obtained in [1] for  $\vartheta = 90^\circ$  and  $\vartheta = 0$ , respectively.

With the definitions of the domain widths  $D_H$  and  $D_G$  for the respective domain structures as given in [1], Figs I.4*b* and *c*, the results of our present measurements are those given in Table I and lead to the curves plotted in Fig. 7.

### 3. Conclusions

The curves from Fig. 7 agree very well with those obtained in [1], including the values of the critical thicknesses  $T_0$  and  $T_1$  which for cobalt are

$$T_0 \approx 12 \mu\text{m}, \quad T_1 \approx 50 \mu\text{m}. \quad (7)$$

Thus, the formula (4) for cobalt is finally proven to be correct and applicable to crystals with (linearly) varying as well as constant  $T$ .

Now, for each domain structure  $X$  (where  $X = H$  or  $G$ ) there are generally four constants in Eq. (4) to be determined from experiment, namely,  $b_m$  and  $a_{X;m}$ . However, it is easily seen from the curves in Fig. 7 that, if  $T_1$  is known, only three of these constants are independent.

Indeed, since

$$D_{X;1}(T_1) = D_{X;2}(T_1) \quad (8)$$

we have from Eq. (4) the relation

$$T_1^{b_1} a_{X;1} = T_1^{b_2} a_{X;2} \quad (9)$$

which permits any of the five constants  $T_1$ ,  $b_m$  and  $a_{X;m}$  to be determined if the remaining four are known. Since  $T_1$ ,  $b_m$  and  $a_{X;1}$  can be determined quite accurately from the diagrams, we use Eq. (9) in calculating  $a_{X;2}$ . The best estimates from large-scale diagrams of our present measurements lead to the values

$$\begin{aligned} T_1 &= 50 \mu\text{m}, & b_1 &= 0.50, & b_2 &= 0.57 \\ a_{X;1} &= \begin{cases} 1.01 & \text{for } X = H \\ 0.66 & \text{for } X = G \end{cases} \quad (\text{in } \mu\text{m}^{0.5}) \end{aligned} \quad (10)$$

which, by virtue of Eq. (9) lead to

$$a_{X;2} = \begin{cases} 0.768 & \text{for } X = H \\ 0.502 & \text{for } X = G \end{cases} \quad (\text{in } \mu\text{m}^{0.43}) \quad (11)$$

in very good agreement with the values (3) as estimated in [1].

The results obtained here and in [1] show that observations and measurements on wedge-shaped samples are quite reliable, at least as far as the determination of the critical thicknesses

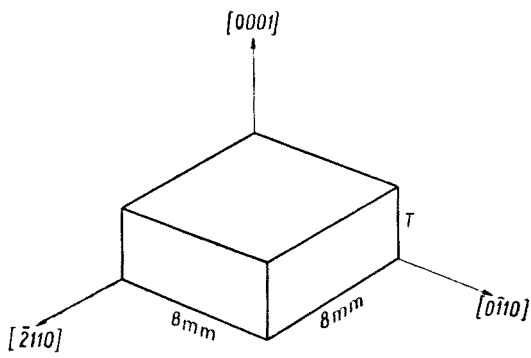


Fig. 1. Shape, size and crystallographic orientation of samples used in the experiment. Thickness  $T$  varying from  $11500 \mu\text{m}$  to  $3 \mu\text{m}$

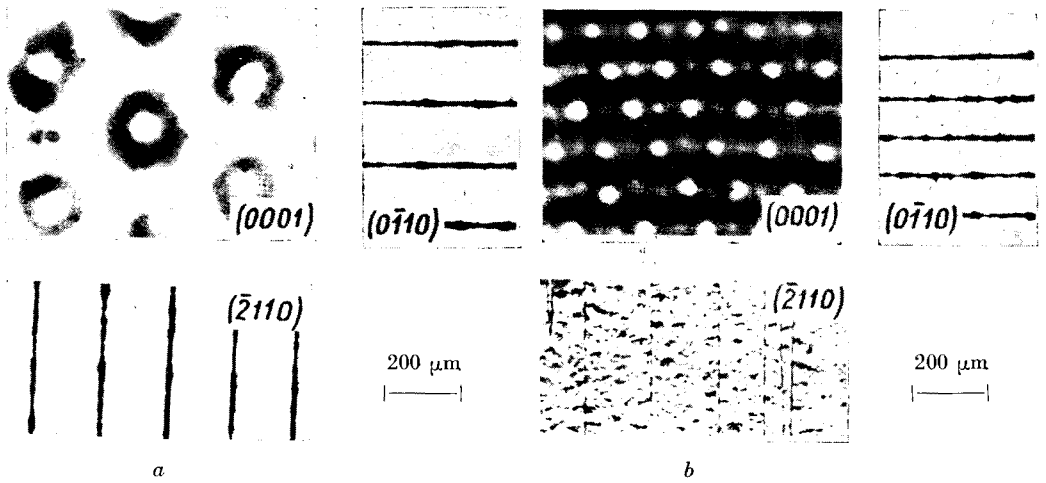


Fig. 2. Powder-patterns on the basal (0001) and axial ( $0\bar{1}10$ ), ( $\bar{2}110$ ) crystal surfaces: *a*. — honeycomb (*H*) and *b* — Goodenough (*G*) domain structure (*cp.* Figs 4, 5). Crystal thickness  $T = 11500 \mu\text{m}$ . Thickness of plastic coating on the basal surface  $38 \mu\text{m}$  (see [4, 15])

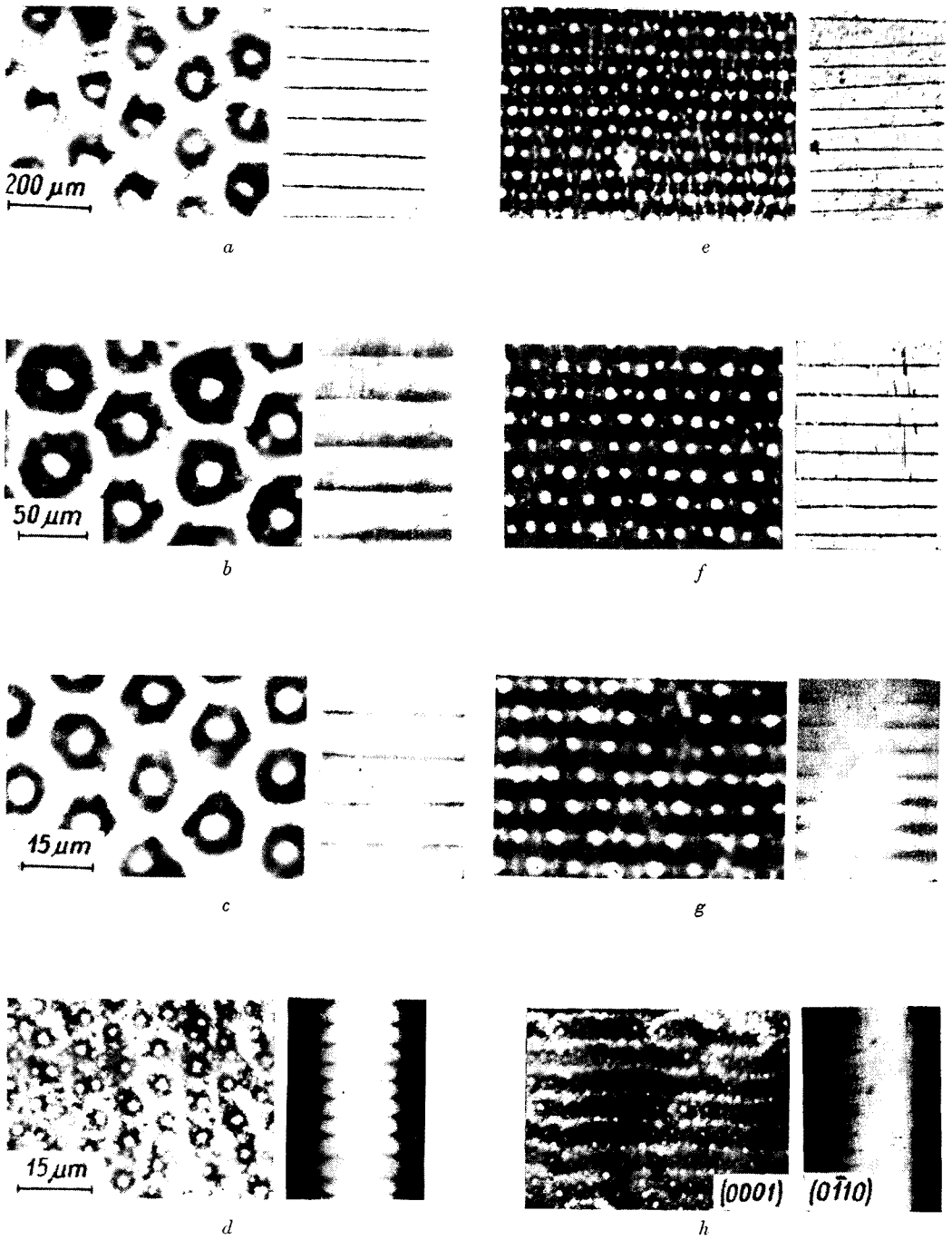


Fig. 3. Powder-patterns on the basal (0001) and axial (0110) crystal surfaces: *a-d* honeycomb (*H*) and *e-h* Goodenough (*G*) domain structure (cp. Figs 4, 5). Crystal thicknesses (from the top): 3700  $\mu\text{m}$ , 850  $\mu\text{m}$ , 77  $\mu\text{m}$ , 15  $\mu\text{m}$ . Thickness of plastic coating: *a, e* - 18  $\mu\text{m}$  *b, f* - 10  $\mu\text{m}$  *c, g* - 4  $\mu\text{m}$  (see [4, 15])



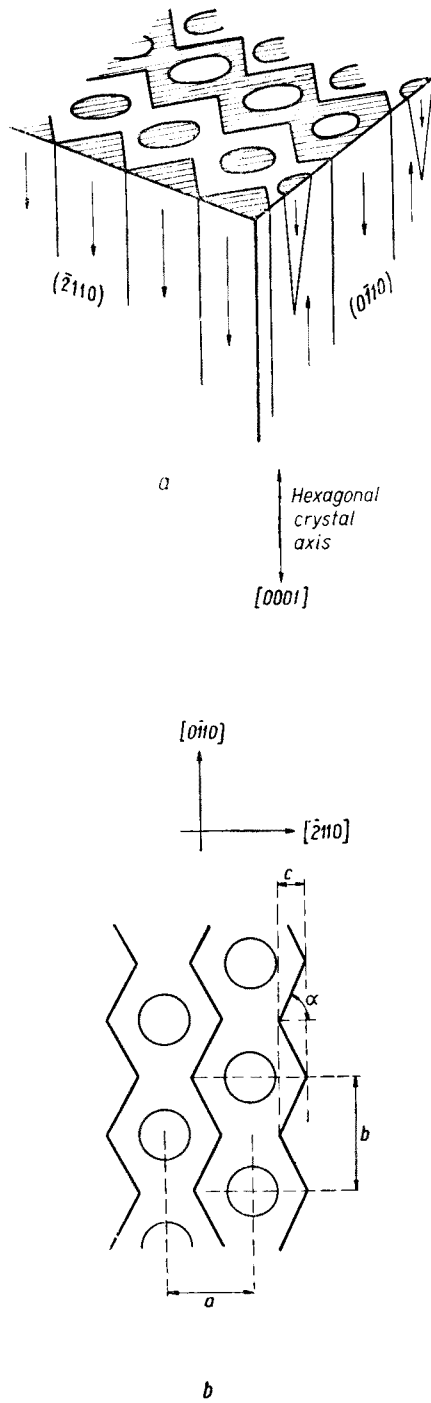


Fig. 5. Model of Goodenough (G) domain structure. Observations show that  $b \approx 1.8a$  and  $\alpha \approx 70^\circ$  (see [3, 4]) which leads to  $c \approx 0.33a$ , in disagreement with theory [5]

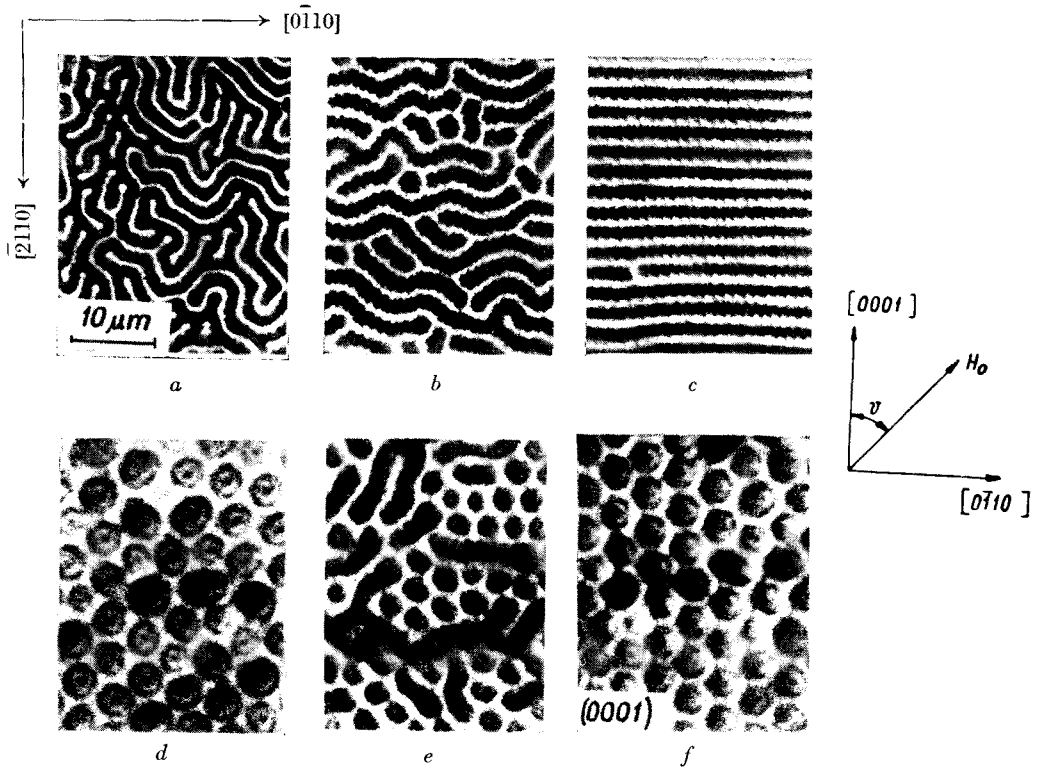


Fig. 6. Powder-patterns on the basal surface (0001) of a thin ( $T = 10\mu\text{m} < T_0 \cong 12\mu\text{m}$ ) sample showing the dependence of the remanent domain structure on the direction of the creating field  $H_0$ . The angle  $\vartheta$  is  $0^\circ$ ,  $40^\circ$ ,  $75^\circ$ ,  $88^\circ$ ,  $90^\circ$  and  $92^\circ$  in  $a$ ,  $b$ ,  $c$ ,  $d$ ,  $e$  and  $f$ , respectively

$T_1$ ,  $T_0$  and the thickness dependence of the domain width are concerned. This is certainly an advantage from the practical view-point, since in this way toilsome experiments on sets of single-crystalline samples can be avoided. On the other hand, the present paper confirms the disagreement between theory and experiment pointed out in [1, 2] and provides further evidence supporting the critique given in [1, 2] of the conclusions arrived at by other authors [6, 8-14].

Finally, we may mention that preliminary results obtained from analogous experiments on non-remanent domain structures in FeSi wedge-shaped single-crystalline samples confirm the relationship (4) between the domain width and the crystal thickness, leading to the values  $T_1 \approx 450 \mu\text{m}$ ,  $b_1 \approx 0.5$ ,  $b_2 \approx 0.9$  which in all likelihood are again independent of the type of domain structure. This would indicate that the rule (4) is generally valid, the exponent  $b_1 = 0.5$  depending neither on the material nor on the type of domain structure, the exponent  $b_2$  and the critical thickness  $T_1$  depending on the material but not on the domain structure, and the coefficients  $a_{x;m}$  depending on both the material and the domain structure.

#### REFERENCES

- [1] B. Wysłocki, *Acta Phys. Polon.*, **34**, 327 (1968).
- [2] B. Wysłocki, W. J. Ziętek, *Acta Phys. Polon.*, **35**, 117 (1968).
- [3] B. Wysłocki, *Acta Phys. Polon.*, **27**, 783 and 955 (1965).
- [4] B. Wysłocki, W. J. Ziętek, *Acta Phys. Polon.*, **29**, 223 (1966).
- [5] G. Kozłowski, W. J. Ziętek, *Acta Phys. Polon.*, **29**, 261 (1966).
- [6] J. Kaczér, R. Gemperle, *Czech. J. Phys.*, B, **11**, 510 (1961).
- [7] H. Kojima, K. Gotō, *J. Phys. Soc. Japan*, **36**, 538 (1965).
- [8] W. Andrä, *Ann. Phys.* (Germany), **1**, 135 (1954).
- [9] G. S. Kandaurova, J. S. Shur, F. V. Maslennikova, *Zh. Eksper. Teor. Fiz.* (USSR), **38**, 60 (1960).
- [10] Y. Takata, *J. Phys. Soc. Japan*, **18**, 87 (1963).
- [11] R. Gemperle, A. Gemperle, I. Bursuc, *Phys. Status Solidi* (Germany), **3**, 2101 (1963).
- [12] J. Kaczér, *Zh. Eksper. Teor. Fiz.* (USSR), **46**, 1787 (1964).
- [13] R. Gemperle, *Phys. Status Solidi* (Germany), **6**, 89 (1964).
- [14] A. Hubert, *Phys. Status Solidi* (Germany), **22**, 709 (1967).
- [15] B. Wysłocki, *Ann. Phys.* (Germany), **13**, 109 (1964).